Steel and Composite Structures, *Vol. 31, No. 1* (*2019*) *85-98*
DOI: https://doi.org/10.12989/scs.2019.31.1.085

Nonlinear seismic performance of code designed perforated steel plate shear walls

Kallol Barua [a] and Anjan K. Bhowmick*

Department of Building, Civil and Environmental Engineering, Concordia University, Montreal, Canada

(*Received June 8, 2018, Revised February 15, 2019, Accepted March 19, 2019*)

Abstract. Nonlinear seismic performances of code designed Perforated Steel Plate Shear Walls (P-SPSW) were studied. Three multi-storey (4-, 8-, and 12-storey) P-SPSWs were designed according to Canadian seismic provisions and their performance was evaluated using time history analysis for ground motions compatible with Vancouver response spectrum. The selected code designed P-SPSWs exhibited excellent seismic performance with high ductility and strength. The current code equation was found to provide a good estimation of the shear strength of the perforated infill plate, especially when the infill plate is yielded. The applicability of the strip model, originally proposed for solid infill plate, was also evaluated for P-SPSW and two different strip models were studied. It was observed that the strip model with strip widths equal to center to center diagonal distance between each perforation line could reasonably predict the inelastic behavior of unstiffened P-SPSWs. The strip model slightly underestimated the initial stiffness; however, the ultimate strength was predicted well. Furthermore, applicability of simple shear-flexure beam model for determination of fundamental periods of P-SPSWs was studied.

Keywords: steel plate shear wall; seismic analysis; perforations; strip model; unstiffened steel plate

1. Introduction

Over the last two decades, unstiffened steel plate shear wall (SPSW) has become a popular lateral load resisting system for wind and earthquakes. Though SPSW can be stiffened and unstiffened, in North America unstiffened SPSW is popular, mainly due to its less fabrication cost. High initial stiffness, excellent ductility and energy dissipation capacity and tremendous post-buckling strength of infill plate make unstiffened SPSW a unique lateral load resisting system. Thorburn *et al*. (1983) first proposed a strip model for analysing thin unstiffened SPSW considering the post-buckling strength in the infill plate. When designing unstiffened SPSW, it is considered that column overturning moment will be resisted by axial coupling loads in columns and storey shear will be resisted by the tension field developed in the infill plate once the plate is buckled.

Research has shown that infill plate thickness requirement for SPSW to resist storey shear is usually low, especially for mid-to-low rise buildings (Bhowmick *et al*. 2009). From availability and constructability point of view it is often observed that the minimum infill thickness used in SPSW is larger than the required plate thickness. When larger than required infill plate thickness is used, it places much higher demand on the seismic load path, making SPSWs less attractive to the structural design community. To overcome this problem researchers have proposed few alternatives. Light-gauge shear walls with cold rolled infill plate can be a viable alternative to improve the economy of the SPSW system (Berman and Bruneau 2005). Another alternative recently put forward is to have circular perforations (Vian 2005, Purba 2006, Bhowmick *et al*. 2014, Shekastehband *et al*. 2017, Ali *et al*. 2018) and rectangular opening (Sabouri-Ghomi *et al*. 2016, Sabouri-Ghomi and Mamazizi 2015, Barkhordari *et al*. 2014, Hosseinzadeh and Tehranizadeh 2012) in the infill plate. Use of low yield strength steel plate shear walls (Soltani *et al*. 2017) can also significantly reduce strength demand of boundary framing members. Among these alternatives, perforated steel plate shear wall (P-SPSW) system has gained wide acceptance to the engineering community. This is because the perforated system can accommodate passing of utilities like electric lines, water pipes, etc. through the infill plate. Also, during construction, lifting and handling of the infill plate becomes easy as well.

Roberts and Sabouri-Ghomi (1992) was the pioneer in research on circular perforations in shear panels. They tested a series of unstiffened steel shear panels with circular perforations at the center of the panels. Based on their quasi-static cyclic tests they proposed a relation between strength of solid steel shear panel and shear panel with a circular perforation

$$V_{op} = V_p\left(1 - \frac{D}{d_p}\right) \tag{1}$$

where V_{op} and V_p are the strength of a perforated and a solid shear panel, respectively, D is the perforation diameter, and d_p is the panel height.

*Corresponding author, Ph.D.,
E-mail: anjan.bhowmick@concordia.ca
[a] M.A.Sc.

ISSN: 1229-9367 (Print), 1598-6233 (Online)

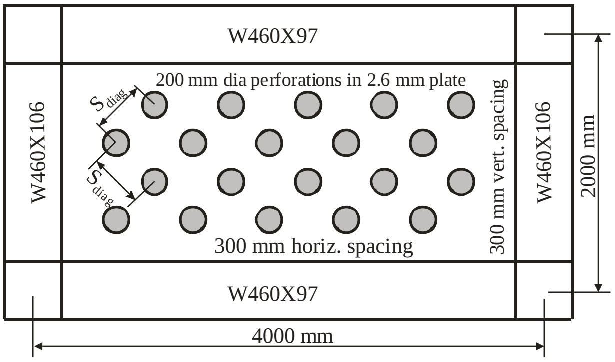

Fig. 1 Perforation layout of test specimen from Vian (2005)

Vian (2005) tested one single storey SPSW with multiple regularly-spaced circular perforations of equal diameter in the infill plate. Later, Purba (2006) conducted analysis of a series of individual strips with regularly spaced circular perforations proposed by Vian (2005). Purba (2006) also analysed a series of single storey SPSWs with proposed regular perforation pattern. It was observed that for the regularly-spaced perforation pattern proposed by Vian (2005), Eq. (1) would provide a conservative estimate of the strength of the perforated infill plate if d_p in Eq. (1) is replaced by S_{diag}, the diagonal distance between each perforation line (as shown in Fig. 1). Based on the analysis the following equation was proposed

$$V_{op} = V_p \left(1 - 0.7 \frac{D}{S_{diag}}\right) \tag{2}$$

Both CSA/CAN S16-09 and AISC 2010 adopted the regular perforation pattern proposed by Vian (2005) in their design standards and have design guidelines for this perforated SPSW system. The same guidelines for design of P-SPSWs have been retained in the current editions of the North American standards (CSA S16-14 and ANSI/AISC 341-16). According to CSA S16-14, openings should be spread uniformly over the entire plate in a staggered position with a certain distance from the boundary (Fig. 1). The openings are oriented in such a way that the plate buckling is independent of loading direction.

Both CSA S16 and AISC requires that P-SPSW be deigned according to the capacity design approach. As per capacity design approach, for P-SPSW, yielding of infill plate and plastic hinging at the end of beams are considered as ductile fuses, where most of the seismic energy is dissipated. However, to the best of these researchers' knowledge, the proposed P-SPSW system has never been studied under real seismic loading. Thus, the objective of this research is to study the seismic performance of code designed P-SPSW system.

Analysis of steel plate shear walls (SPSWs) using detailed FE model is very time-consuming and design engineers prefer to use a simplified technique, called strip model, to analyse SPSW. Modified strip model suggested by Shishkin *et al*. (2005) is an effective tool for performance assessment of SPSW with solid infill plate. The applicability of the modified strip model to assess inelastic responses of P-SPSWs is not known to structural engineers. This paper investigates applicability of modified strip model for analysis of P-SPSWs. Strip models with two different strip widths were considered. The proposed strip model has been used in conventional software, SAP2000, to estimate inelastic responses of the selected 4-, 8, and 12-storey P-SPSWs.

Seismic provisions in building codes require accurate estimation of the fundamental period for calculating earthquake design base shear and lateral forces in every storey. This often asks for development of detailed finite element models of P-SPSWs, which is a time consuming process. Bhowmick *et al*. (2011) previously investigated effectiveness of a simple shear-flexure cantilever model to determine fundamental periods of solid SPSWs. Similar approach has been used in this paper for P-SPSW and applicability of using the simple shear-flexure beam model, instead of a full P-SPSW model, to determine the fundamental periods of P-SPSWs is also studied in this paper.

2. Finite element (FE) modeling of P-SPSW

A nonlinear finite element model was developed using comprehensive FE software ABAQUS. The FE model was validated against experimental results by Vian (2005). Both material and geometric non-linarites were considered in the FE model to capture the actual post-buckling behavior of the unstiffened P-SPSW.

2.1 Characteristics of FE model

For the FE model, fish plates were neglected and it was considered that infill plate was directly welded with surrounding boundary members. For initial imperfection corresponding first buckling mode of the infill plate was included with a scale factor of respective plate thickness. Appropriate mesh size is an integral part of FE analysis. Multiple openings made the perforated infill plate area very complex for meshing. Mesh convergence study was conducted to select the proper mesh size. In this study, shell element (ABAQUS element S4R) was used for both infill plates and boundary members. In four node shell element (S4R), each node has six degrees of freedoms: three translations (ux, uy, uz) and three rotations (θx, θy, θz).

The yield stress for boundary elements and infill plates was taken as 350 MPa and 385 MPa, respectively. Moreover, corresponding elastic modulus (E) and Poison's ratio (ν) were taken as 200 GPa and 0.3, respectively. For the seismic analysis, Rayleigh proportional damping with a ratio of 5% was selected. Also, the storey gravity loads were represented as lumped masses on the columns at every floor. To model pin supports, reference points (RP) were created at the bottom of each column. Connections between RP and base nodes of the column were obtained by connector element (CONN3D2). Boundary conditions (pin support) were employed at the respective reference point (RP). During seismic analysis, horizontal movement at the reference points was released. The out-of-plane movement was restrained in the panel zones. When doing the seismic analysis, one dummy column was added to the P-SPSW to simulate gravity columns. The connections between the P-SPSW and the dummy column were provided by rigid links in every storey.

2.2 Validation of the FE model

The FE model was validated for the regularly spaced perforated SPSW test by Vian (2005). The specimen tested by Vian (2005) was a single-bay, single-storey SPSW with a geometry of 4000 mm wide by 2000 mm high and had rigid beam-to-column connections. For this test, beams and columns had specified yield strength of $F_y = 345$ MPa. The infill plate used had a thickness of 2.6 mm and had yield strength and ultimate strength of 165 MPa and 305 MPa, respectively. A displacement controlled pushover and quasi-static cyclic analysis was conducted. Fig. 2 shows the FE mesh of the test specimen. The pushover curve obtained from nonlinear static analysis, as shown in Fig. 3, shows that sufficient agreement was obtained with test results. Initial stiffness exactly matched with experiment but ultimate strength was slightly underestimated (around 3%). The hysteresis behavior from the cyclic analysis is shown in Fig. 4 and a good correlation with experimental results is obtained. Thus, it can be concluded that the developed FE model is capable of predicting the behavior of P-SPSW.

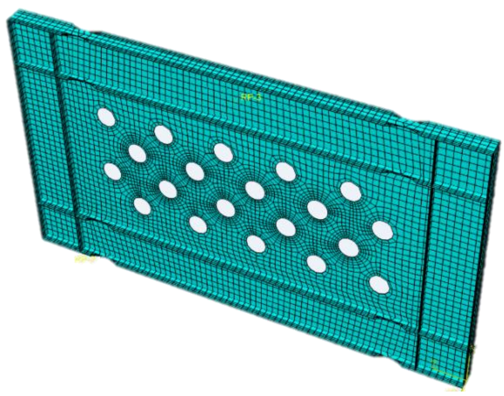

Fig. 2 FE mesh of Vian (2005) test specimen

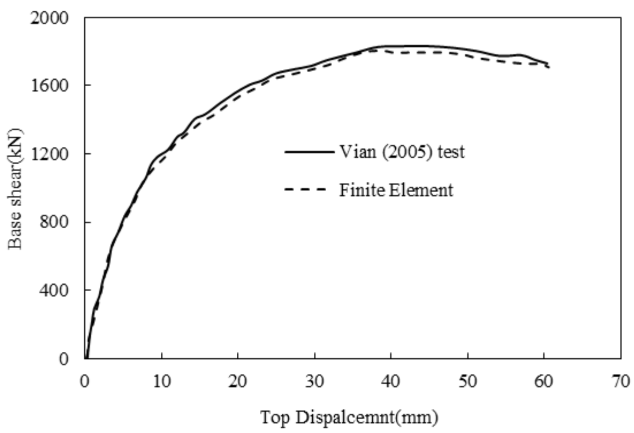

Fig. 3 Force-displacement curves of the Vian (2005) test and FE analysis

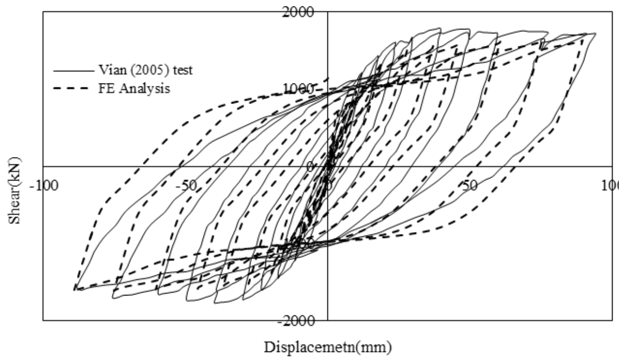

Fig. 4 Hysteresis curves of the test specimen of Vian (2005) and FE analysis

3. Analysis of perforated steel plate shear walls

Nonlinear finite element analyses of three multi-storey P-SPSWs with code specified regular circular perforations were carried out using ABAQUS. Both nonlinear static and seismic analysis were conducted.

3.1 Selection of multi-storey P-SPSWs

A set of three office buildings with 4-, 8-, and 12- storey were selected for this study. The hypothetical office buildings were assumed to be located in Vancouver, BC. The buildings had regular plan area of 2631.7 m^2 (as shown in Fig. 5) and had two identical ductile perforated SPSWs in both directions (N-S, E-W). The typical elevation views of the P-SPSWs are shown in Fig. 6. Even though the building was symmetric over the height as well as in plan, accidental torsion was considered during earthquake load calculation.

The chosen building had equal storey height of 3.8 m and a bay width of 5.7 m in all directions (aspect ratio of 1.5 for all selected P-SPSWs). The foundations were assumed to be on very dense soil or soft rock (site class C according to NBCC 2010). For every floor a 4.2 kPa of dead load and a live load of 2.4 kPa were considered. For roof level 1.5 kPa of dead load and 1.12 kPa of snow load were considered. For seismic load calculation, full dead load with 25% snow load was considered. The load combinations of 1.0D + 0.5LL + 1.0E (where D = dead load; LL = live load; E = earthquake load) and 1.0D + 0.25S + 1.0E (where S = snow load) were used for designing beams and columns at floor and roof level respectively. The factored shear resistance of infill plates with circular perforations can be calculated as per Eq. (3), provided by CSA/CAN-S01-09.

$$V_r = 0.4\,(1 - 0.7\frac{D}{Sdiag})\emptyset F_{py}\, t_w L sin2\alpha \tag{3}$$

where V_r = is the storey shear, α = the angle of inclination of the tension field, t_w = thickness of the infill plate, L = plate width, $\emptyset$ = resistance factor, taken as 0.9, S_{diag} = shortest centre-to-centre distance between the perforations, D = perforation diameter.

To form appropriate tension field action in the infill plates, holes' positions are very critical for any perforated

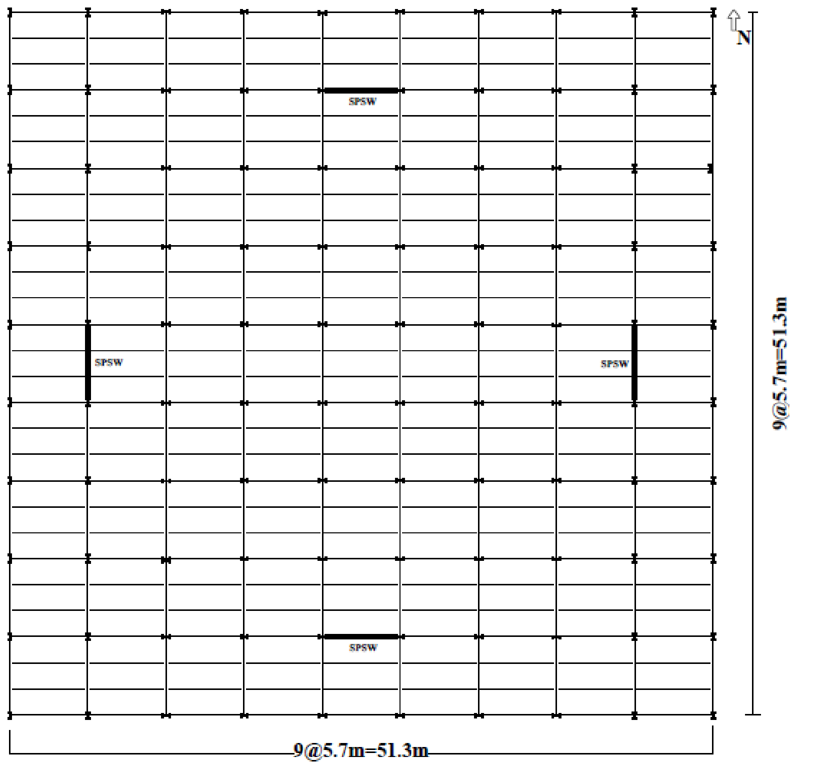

Fig. 5 Typical floor plan of the hypothetical office building

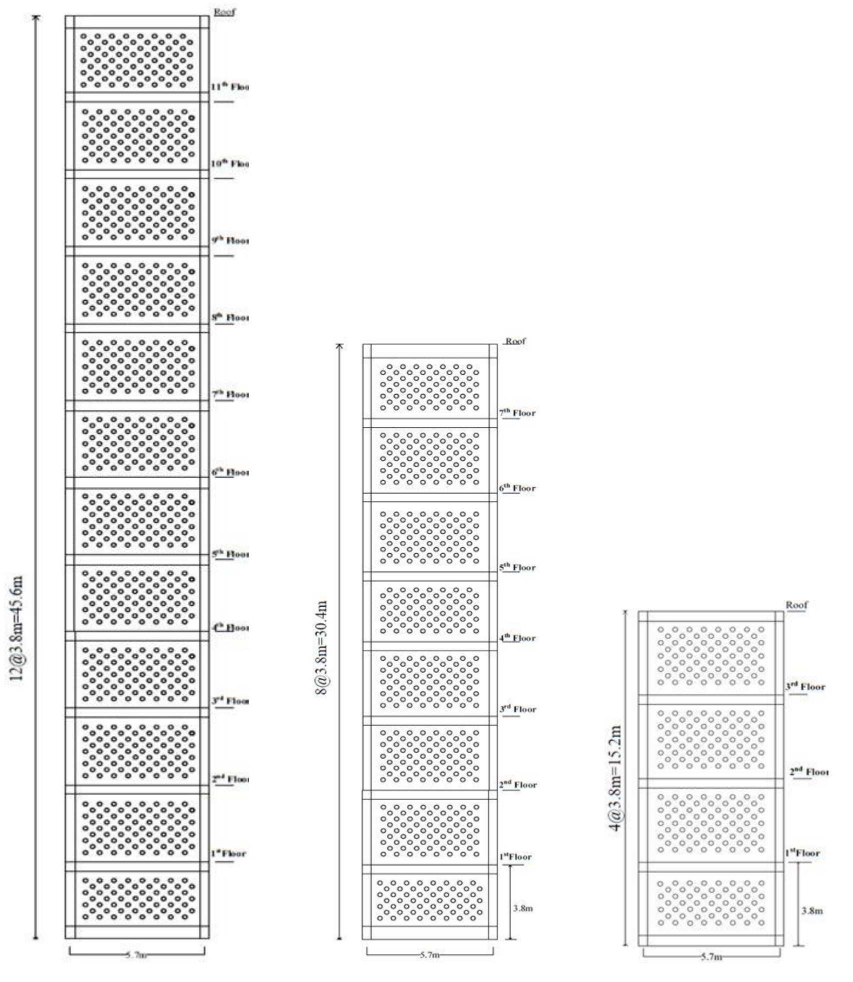

Fig. 6 Elevation view of the P- SPSW (a) 12-storey (b) 8-storey and (c) 4-storey

SPSW. For multiple openings, it is recommended in CSA/CAN-S16-09 that the openings should be uniformly distributed over the entire plate with staggered position. The openings of 200 mm diameters along with 300 mm C/C distance between perforations were considered in this study. Thus, the diagonal strip width (S_{diag}) of 424.24 mm (D/S_{diag} = 0.47) was used. Also, an edge distance between diameter (D) and D + $0.7S_{diag}$ was maintained from the boundary members to a perforation. For designing vertical boundary members, capacity design procedure provided by Berman and Bruneau (2008) was followed. Even though Berman and Bruneau (2008) proposed the procedure for solid infill, it is equally applicable to perforated one. Fully yielded infill plates with plastic hinges at the ends of each beam were considered during uniform collapse mechanism. The beams and columns were designed to carry the yielding forces of the infill plates. Tables 1, 2, and 3 present the details of the selected 4-, 8-, and 12- storey P-SPSWs.

A minimum infill plate thickness of 3.0 mm was used in this research, as this was considered the minimum practical thickness using conventional welding practice and for handling considerations. Shishkin *et al*. (2005) observed that the ultimate base shears of SPSWs varied little when the angle of inclination of the tension field, α, was changed from 38° to 50°. Also, at the beginning of design of any SPSW, the column sections are unknown to determine the angle of tension field. Thus, the value of the angle of the diagonal tension field was assumed as 45° in this paper. With the angle of the tension field known, boundary beams and columns were selected. The top and bottom beams were selected to anchor the tension forces from the yielded infill plate. Also the column sections were selected to carry the forces developed in the yielded infill plate and the plastic hinges at the ends of the top beams. CAN/CSA-S16-09 also has provisions for the stiffness of the columns to ensure the development of an essentially uniform tension field in the infill plate. The required limit on the flexibility parameter, ω_h, is given as

$$\omega_h = 0.7h\sqrt[4]{\frac{w}{2LI_c}} \leq 2.5 \qquad (4)$$

where w is the infill plate thickness; L is the bay width; h is the storey height; and I_c is the moment of inertia of each column.

Table 1 Summary of 4-storey P-SPSW

Floor level	Plate thickness (mm)	Opening diameter (mm)	Beam section	Column section
Roof	3	200	W460X315	W360X314
Floor-3	3	200	W460X144	W360X314
Floor-2	3	200	W460X144	W360X509
Floor-1	3	200	W460X144	W360X509
Bottom			W460X315	W360X509

Table 2 Summary of 8-storey P-SPSW

Floor level	Plate thickness (mm)	Opening diameter (mm)	Beam section	Column section
Roof	3	200	W610X415	W360X463
Floor-7	3	200	W460X144	W360X463
Floor-6	3	200	W460X144	W360X634
Floor-5	3	200	W460X144	W360X634
Floor-4	3	200	W460X144	W360X634
Floor-3	4.8	200	W460X144	W360X634
Floor-2	4.8	200	W460X260	W360X900
Floor-1	4.8	200	W460X260	W360X900
Bottom			W610X415	W360X900

Table 3 Summary of 12-storey P-SPSW

Floor level	Plate thickness (mm)	Opening diameter (mm)	Beam section	Column section
Roof	3	200	W610X341	W360X421
Floor-11	3	200	W460X144	W360X421
Floor-10	3	200	W460X144	W360X421
Floor-9	3	200	W460X144	W360X421
Floor-8	3	200	W460X158	W360X634
Floor-7	3	200	W460X158	W360X634
Floor-6	3	200	W460X213	W360X634
Floor-5	4.8	200	W460X213	W360X634
Floor-4	4.8	200	W460X260	W360X1086
Floor-3	4.8	200	W460X260	W360X1086
Floor-2	4.8	200	W460X384	W360X1086
Floor-1	4.8	200	W460X384	W360X1086
Bottom			W610X415	W360X1086

3.2 Pushover analysis and results

Before seismic analysis, nonlinear pushover analysis was conducted for each of the selected P-SPSWs. Earthquake lateral loads obtained from equivalent static load procedure in NBCC 2010 were considered for the pushover analysis. Linear perturbation buckling analysis was performed to incorporate the initial imperfection in the respective infill plate. The lateral loads were increased monotonically during the pushover analysis. It was observed that for all the P-SPSWs, tension field action fully developed before yielding of the infill plates. Plastic hinges were formed at the end of the beams after yielding of infill plates. Plastic hinges also formed at the base of the columns. Thus, all the P-SPSWs performed as per capacity designed. Table 4 compares the base shears obtained from the equivalent lateral force method in NBCC 2010 and that from nonlinear pushover analysis. For the 4-, 8- and 12-storey P-SPSWs static base shears from pushover analyses were 172%, 67%, and 140% higher than the design base

Table 4 Comparison of base shear from NBCC 2010 and pushover analysis

P-SPSW	Base shear (kN)	
	NBCC 2010	Pushover analysis
4-storey	1508	4110
8-Storey	2970	4950
12-storey	3354	8076

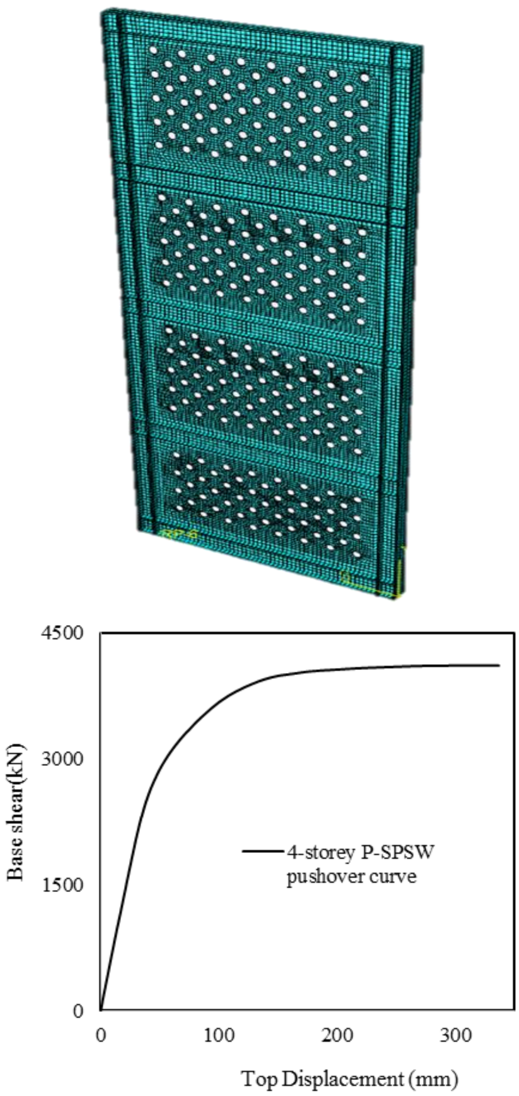

Fig. 7 Four storey P-SPSW FE mesh and pushover analysis results

shears from NBCC 2010. This is mainly due to use of larger than required infill plate thickness. When higher overstrength infill plates are used, steel plate shear walls require very heavier boundary columns to be designed to achieve full capacity of the infill plates. Also, during design, the column shear contribution was neglected, but in practice a considerable amount shear is taken by the columns. Fig. 7 shows a typical finite element mesh for 4-storey P-SPSW. Fig. 7 also shows the pushover curve for the selected 4-storey perforated SPSW.

4. Seismic response of perforated steel plate shear wall (P-SPSW)

In addition to nonlinear static pushover analysis, seismic analyses of the selected three multi-storey P-SPSWs were conducted. The objective of dynamic time history analysis was to assess the performance during the earthquake. Also, NBCC 2010 recommends use of dynamic time history analysis for structures with fundamental time periods more than 2 seconds, which is the case for the selected 12-srorey P-SPSW.

4.1 Frequency analysis

Frequency analyses of the selected three P-SPSWs were conducted to estimate the fundamental periods of the shear walls. Fundamental periods were later used to determine the scaling factors for the selected ground motion records. In addition, fundamental periods are required to calculate the Rayleigh proportional damping coefficients α and β. A 5% Rayleigh proportional damping factor was considered.

For the frequency analysis an additional dummy column was added parallel to the P-SPSW in the FE model. The dummy column was used to account for the P-Δ effect of the surrounding gravity columns. Two node 3D truss element (ABAQUS T2D3) was used with a link connection between the stories to dummy column. The material properties of the dummy column were considered similar to the material properties of boundary columns. Moreover, half of the building’s lumped masses were added in the dummy column at the respective storey level. For P-SPSW, the lumped masses were applied at the top of each column. Frequency analysis was conducted for 4-, 8-, and 12-storey P-SPSWs and corresponding first two modes of vibrations were estimated. Frequencies of the first and second mode of vibrations are given in Table 5.

4.2 Selection of earthquake records

ASCE 7-10 (2010) recommends a minimum of three ground motion records for time history analysis, when peak maximum response are considered for component checking and a minimum of seven ground motion records when the average of maximum response are considered for component checking. Ten seismic records (six real earthquake records and four simulated records) were selected in this study. Real ground accelerations data were

Table 5 Frequency and corresponding periods of 4-, 8- and 12-storey P-SPSWs

P-SPSW		Frequency (rad/sec)	Period (sec)
4-storey	1^{st} mode	6.20	1.01
	2^{nd} mode	17.16	0.37
8-storey	1^{st} mode	2.97	2.10
	2^{nd} mode	9.39	0.67
12-storey	1^{st} mode	1.92	3.27
	2^{nd} mode	6.58	0.95

taken from Pacific Earthquake Engineering Research Center (PEER 2010); on the other hand, site dependent artificial ground motions data were taken from Engineering Seismology toolbox website (Gail *et al*. 2009). The selected real ground motions were chosen to have A/V (A, peak acceleration in scale of g and V, peak velocity in m/s, where g is acceleration due to gravity in m/s^2) values close to 1 conforming with the A/V value for an earthquake expected in Vancouver (Naumoski *et al*. 2004). Only horizontal component of the ground motion records were selected for this study.

Tables 6 and 7 present some important features of the four real ground motion record and four simulated earthquake records. The simulated earthquakes included two different sets of records having magnitude 6.5 and 7.5 respectively for soil class C. The selected ground motions were scaled based on the partial area method (Naumoski *et al*. 2004) of ground motion scaling. According to this method, the area under the acceleration response spectrum curves of ground motion records between 0.2T to 1.5T; where, T is the fundamental period of vibration of the building, is compared with the area under the design response spectrum of Vancouver in the designated range and made equal by finding out a suitable scaling factor and modifying the concerned accelerogram with that factor. This period range of the excitation motions is assumed to have the largest effects on the structural response. Scaling factors for all the selected earthquakes were calculated and are provided in Tables 6 and 7.

4.3 Seismic responses of selected P-SPSWs

Nonlinear seismic analyses of 4-, 8-, and 12-storey P-SPSWs were conducted for the selected ten earthquake records. From non-linear time history analysis, it was observed that for 4- and 8-storey P-SPSWs, yielding occurred in the infill plates only, and the boundary frames remained essentially elastic. Thus, for the selected P-SPSWs, seismic energy was mainly dissipated through yielding of the infill plates. For the 12-storey P-SPSW, infill plates at lower storeys participated in energy dissipation by yielding and the infill plates at upper floors remained partially elastic.

For all the P-SPSWs, average interstorey drifts (Fig. 8) were less than the code limit. For 12-storey P-SPSW, due to the higher mode effect, the drift demand increased in the upper stories. In addition, the infill plates at the upper levels were designed with overstrengths much greater than those at the lower storeys. Infill plates with high overstrength do not contribute much to the system ductility. Thus, the seismic drift demands on the upper stories are less.

The average dynamic base shears for the selected ground motions were estimated 110%, 230%, and 150% higher than NBCC 2010 static base shears for the 4-, 8- and 12-storey P-SPSWs, respectively. The average seismic shear on every floor was higher than the design storey shear force. One of the main reasons for this was the over-strengths of the selected steel infill plates. Also, as stated earlier, the column shear contribution was neglected during design, but in practice a considerable amount of shear is taken by the columns.

Dynamic shear in the mid-section of the perforated plate was compared with the shear strength equation provided in CAN/CSA S16-09 for perforated steel plate. Fig. 9 presents the dynamic shears in the perforated plates for the three selected perforated shear walls. It is observed that the equation in Canadian steel design standard, CAN/CSA S16-09, overestimates the average shear forces for the three selected P-SPSWs. For the bottom floors the average dynamic shears in the perforated plates were close to the code specified nominal shear strength. This was because the infill plates at the bottom floors were fully yielded. The percentage of variation increases with the rise of the floor level for the selected P-SPSWs. Therefore, the strength

Table 6 Selected real time ground motions records from PEER database

Event	Station	Magnitude	A/V	Scaling Factors		
				4-storey	8-storey	12-storey
Imperial Valley-California, 1979	183 El Centro	6.53	1.04	0.99	1.04	1.01
Kern County, 1952	Taft Lincoln School	7.3	1.02	1.86	1.81	1.89
Kobe city, Japan 1995	1105 HIK	6.6	0.97	1.71	1.57	1.61
Loma Prieto, USA, 1989	739Anderson Dam	6.93	1.05	1.31	1.38	1.47
Northridge, USA, 1994	68 LA-Hollywood Stor FF	6.7	1.2	1.38	1.34	1.42
San Fernando, USA, 1971	68 LA-Hollywood	6.6	1.05	1.61	1.64	1.68

Table 7 Parameters of selected simulated earthquake records

Event name	Magnitude	Distance (Km)	Peak acceleration (cm/s^2)	Scaling factors		
				4-storey	8-storey	12-storey
6C1	6.5	8.8	487	0.7	0.78	0.88
6C2	6.5	14.6	265	1.3	1.48	1.64
7C1	7.5	15.2	509	0.83	0.91	0.97
7C2	7.5	45.7	248	1.66	1.45	1.83

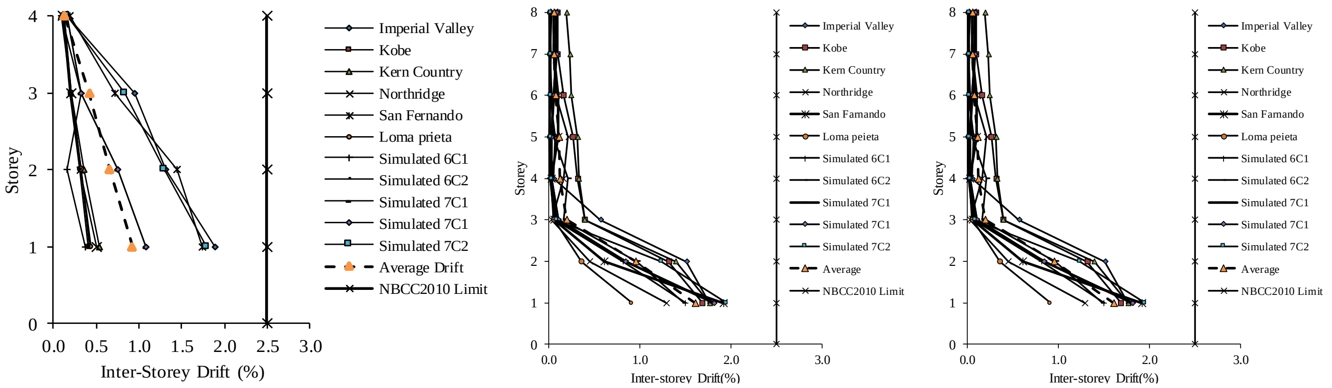

(a) (b) (c)

Fig. 8 Inter-storey drift for (a) 4-storey; (b) 8-storey; and (c) 12-storey P-SPSWs

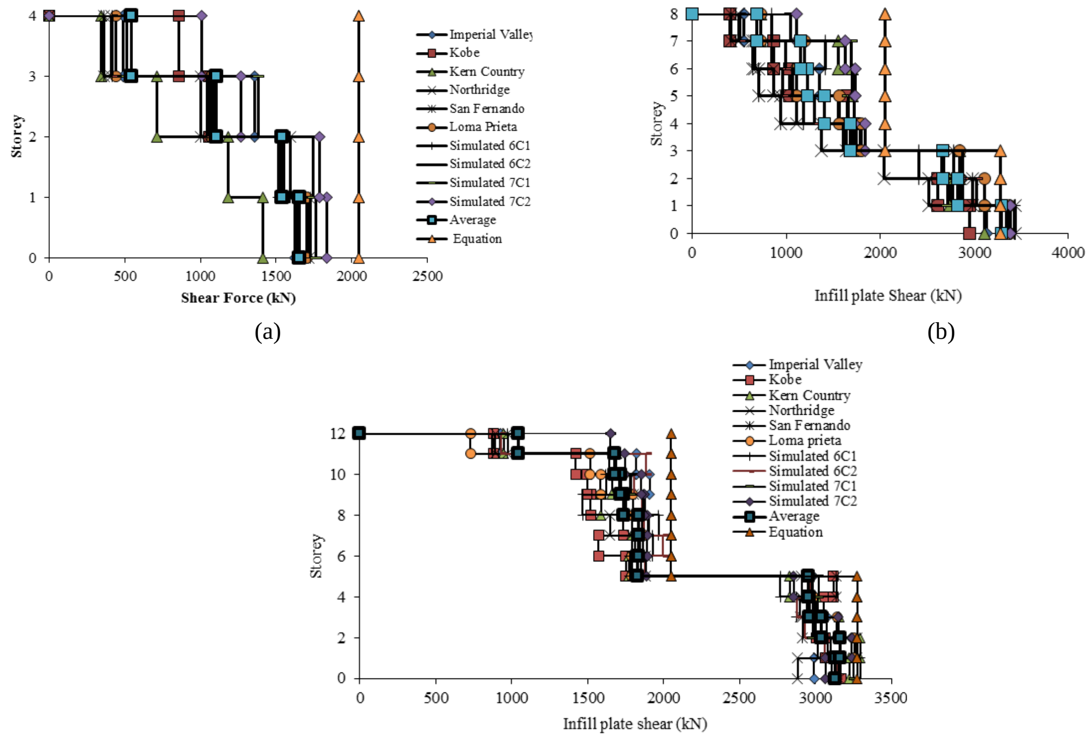

(a) (b)

(c)

Fig. 9 Dynamic shear force in infill plates for (a) 4-storey; (b) 8- storey, and (c) 12-storey P-SPSWs

equation in the standard is safe to use in the design of P-SPSW. It should be noted that although Canadian seismic design provisions have been used, within the scope of the study, the conclusions are considered to be general and apply equally to their U.S. and European counterparts.

5. Modified strip model for perforated steel plate shear walls

Both Canadian and American steel design standards have adopted the strip model for analysis of unstiffened SPSW. Strip model, first proposed by Thorburn *et al.* (1983), is a simple method and is widely used for analysis of unstiffened SPSW. Shishkin *et al.* (2005) proposed modified strip model (MSM) to make a better prediction of the experiment results of Driver *et al.* (1998). Modified strip model is commonly used for analysis solid steel plate shear walls. In this paper, applicability of modified strip model for perforated steel shear wall is investigated.

5.1 Modeling techniques of modified strip method for P-SPSWs

The modified strip model is developed for commercial use and thus, in this paper, commonly used commercial software SAP2000 was used for modeling and analysis of modified strip model. Similar to the modified strip model, a compression strut opposite to the tension strips was considered in each panel. The area of the compression strut was taken from the equivalent brace model recommended by Thorburn *et al.* (1983). The pin ended compression strut

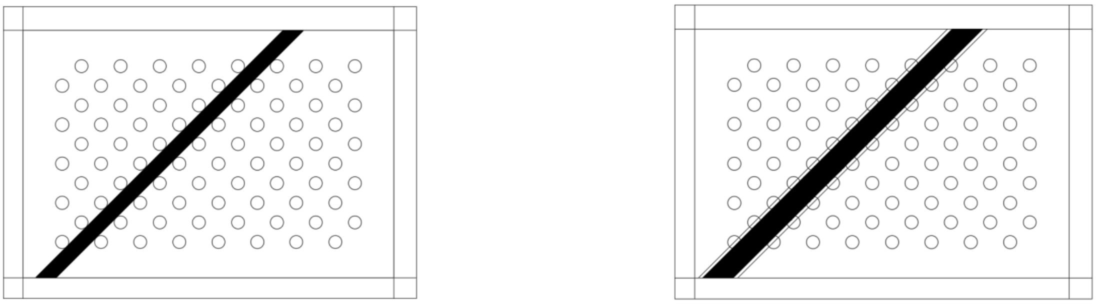

Fig. 10 Tension strips width from edge to edge (E/E) and center to center (C/C)

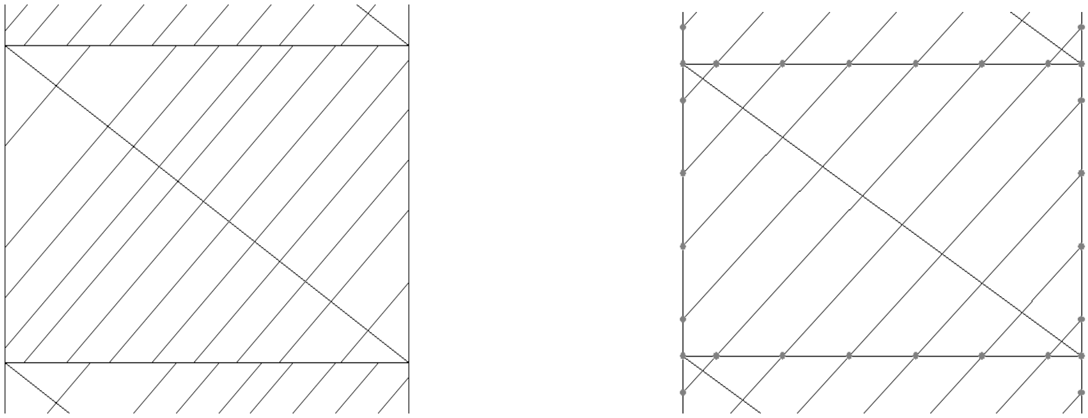

Fig. 11 Tension strips layout: Exact layout (left); Crosshatch layout (right)

was modeled by connecting two opposite corners, and zero tension capacity was assigned to it. As compression strut will be buckled due to the application of the small amount of lateral load, so the material strength of the compression strip was taken 15% of tension strips. The strength was obtained from a sensitivity analysis of the strength of compression strut.

Plastic hinges were incorporated both in frame elements and strips to simulate the inelastic behavior in unstiffened P-SPSW. The plastic hinges were placed at a distance of one-half depth of the particular frame. Hinge properties were taken in such a manner that it could act as perfectly rigid until yielding. The flexural hinges in the beams and columns were symmetric under moment reversal. A small post yielding slope (0.0002:1) was incorporated in the column hinges to attain convergence.

For deterioration hinges, ten times yielding force of the axial hinge was assigned to simulate quick yielding of deterioration strips. The axial hinge properties were considered symmetric. Details of the development of the modified strip model for P-SPSW are presented elsewhere (Barua 2016).

Even though minimum ten strips were required for solid infill plate, for perforated infill plate the number of strips was taken as strips between the diagonal openings (exact layout). In addition, as shown in Fig. 10, two types of strip widths were taken into account: center to center (C/C) and edges to edges (E/E) of perforations. The strips were assigned as zero compressive capacity to take only tensile strength.

In addition, two different strip layouts (Fig. 11) were considered to investigate the behavior of perforated plates. One was exact layout and the other one was crosshatch layout. In crosshatch layout, the upper and lower strips share the same node, whereas, in the exact layout, strips are connected in the actual position of the frame. Fig. 12 presents modified strip model representations with exact layout for 4-storey P-SPSW.

The test specimen by Vian (2005) was considered to validate the accuracy of the developed modified strip model. No gravity load was considered in the model because such kind of load was not applied during the test. The lateral load was applied at the mid-point of the top beam. Mid-point displacement was monitored with corresponding base shear in the pushover curve. From the nonlinear pushover analysis, it was found that the MSM model with C/C strip width was sufficient to predict the elastic to post yielding behavior for the P-SPSW. Initial stiffness was slightly underestimated and ultimate strength was slightly over-predicted in compare to the test (Fig. 13). The variation of ultimate strength was around 5%. On the other hand, MSM model with E/E strip width considerably underestimated both initial stiffness and strength for the load-displacement curve for the test specimen (Fig. 13). Thus, the modified strip model with C/C strip width can be an effective tool for evaluation of the inelastic behavior of P-SPSW.

5.2 Nonlinear pushover analysis of selected P-SPSWs using modified strip model

In order to check the effectiveness of modified strip

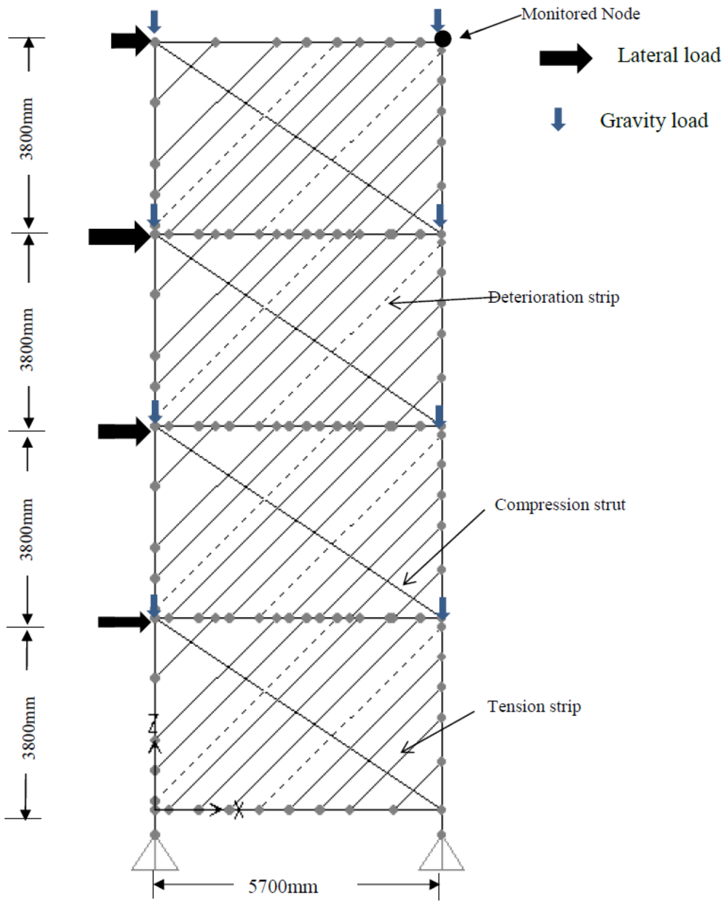

Fig. 12 Modified strip model for 4-storey P-SPSW

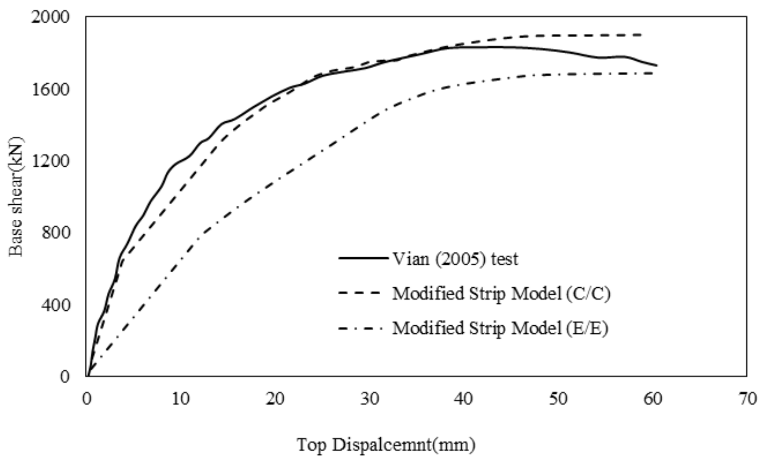

Fig. 13 Pushover curve of Vian (2005) test and Modified Strip Model

model, pushover nonlinear static analyses of the selected 4-, 8- and 12-storey P-SPSWs were conducted. Pushover responses from modified strip models were compared with results from detailed finite element models analysed in ABAQUS. It was observed that the strip model performed very well to capture both elastic and inelastic behavior of the selected P-SPSWs. The model was capable of predicting strength reduction in pushover curve because of distinct modeling of deterioration strip from tension strips. Analysis was conducted separately considering both center to center (C/C), and edge to edge (E/E) strip widths for the 4-storey P-SPSW for exact layout. From the pushover curve in Fig. 14, it can be easily observed that the initial stiffness was slightly underestimated, but the ultimate strength for 4-storey P-SPSW was predicted well. In addition, when compared against the detailed FE model the C/C strip model performed very well in comparison to the E/E strip model. Considering C/C strip width, the performance of the cross-hatch strip layout for the 4-storey P-SPSW was evaluated as well. Form pushover analysis, as shown in

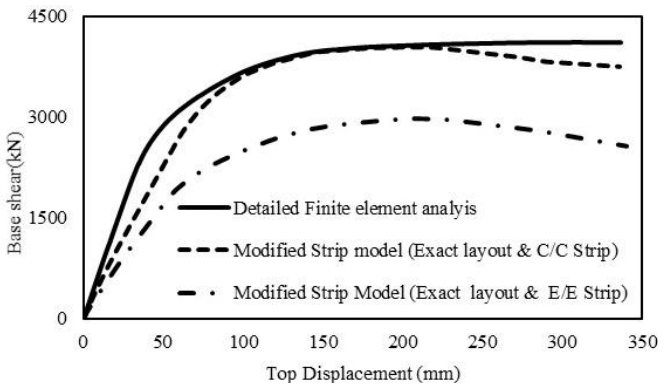

Fig. 14 Base shear versus top displacement for the 4-storey P-SPSW

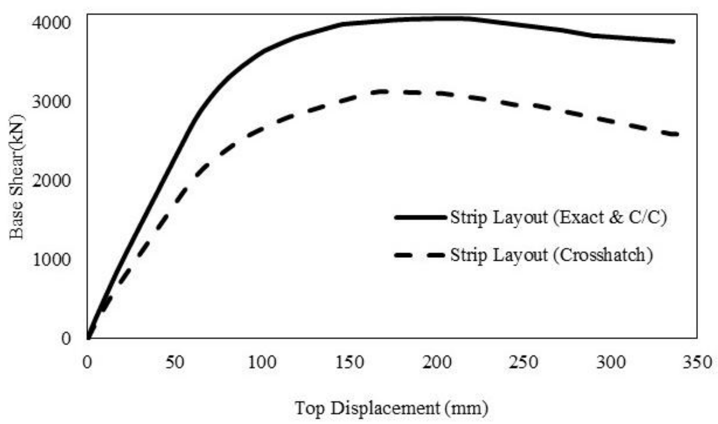

Fig. 15 Pushover curves for different layout of the tension strips for the 4-storey P-SPSW

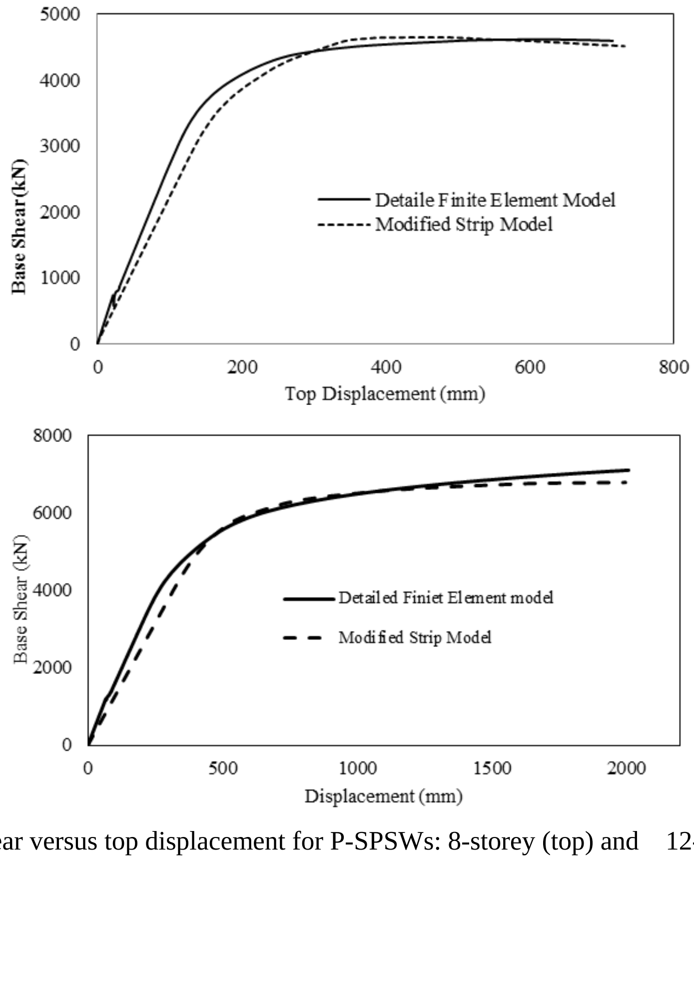

Fig. 16 Base shear versus top displacement for P-SPSWs: 8-storey (top) and 12-storey (bottom)

Fig. 15, it was observed that both stiffness and strength of 4-storey P-SPSW with cross-hatch strip layout were underestimated considerably when compared to results from modified strip model with exact layout. Thus, for 8- and 12-storey P-SPSWs, strip model with only C/C strip width and exact layout was considered. Fig. 16 shows that the modified strip model is in good agreement with results from detailed finite element models for 8-storey and 12-storey P-SPSWs. Similar to 4-storey P-SPSW, for 8- and 12-storey P-SPSW the ultimate strength closely matched, but initial stiffness was slightly under-estimated when compared to detailed analysis results from ABAQUS.

6. Estimation of periods of P-SPSWs using the shear-flexure cantilever model

Research on development and application of shear-flexure beam model to estimate fundamental periods of solid SPSWs was previously done by Topkaya and Kurban (2009) and Bhowmick *et al*. (2011). This model is modified in this paper and its applicability in estimating fundamental periods of P-SPSWs is studied.

A shear-flexure beam model is shown in Fig. 17 for a four-storey P-SPSW. The model has nodes in each floor, which are connected by simple beams. Each node has two degree of freedoms (horizontal and vertical translations). The floor masses are applied at floor levels. Each beam element has both flexural and shear stiffness equivalent to the corresponding P-SPSW storey.

For a simple cantilever beam loaded at the free end with a concentrated transverse load, the effective shear area, A_v, is given by (Charney *et al*. 2005)

$$A_v = \frac{I^2}{\int \frac{Q^2(y)dy}{t(y)}} \tag{5}$$

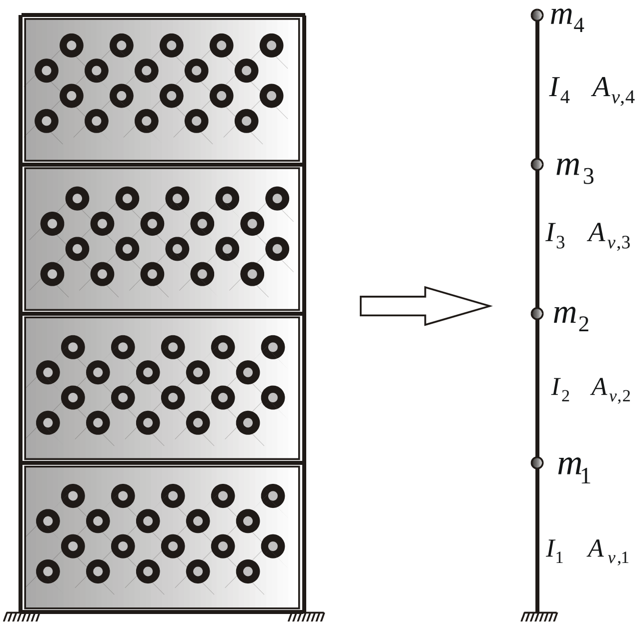

Fig. 17 Shear-flexure cantilever idealization of P-SPSW

where Q is the first moment of the area with respect to the neutral axis and $t(y)$ is the width of the cross section at y. Similarly, the effective shear area of P-SPSW at any storey i can be calculated as

$$A_v = \frac{I_{SW,i}^2}{\int \frac{Q_i^2 dA}{b^2}} = \frac{I_{SW,i}^2}{\beta_i} \tag{6}$$

where $I_{SW,i}$ is the equivalent moment of inertia of the P-SPSW at any storey i, $\beta_i = \int \frac{Q_i^2 dA}{b^2}$ and b is the width of the P-SPSW.

The exact calculation of β_i in Eq. (6) is computationally expensive. Similar to the solid SPSW, as presented previously by Bhowmick *et al*. (2011), at any storey i, the value of β_i can be taken as sum of contributions from boundary columns,$(\beta_1)_i$, and the infill plate, $(\beta_2)_i$.

$$\beta_i = (\beta_1)_i + (\beta_2)_i \tag{7}$$

where

$$(\beta_1)_i = \frac{(Q_1)_i^2 + (Q_2)_i^2}{w_{c,i}} d_{c,i}$$

$$(\beta_2)_i = \frac{(Q_3)_i^2 + (Q_4)_i^2}{2w_{i,eff}} b_w$$

where

$$(Q_1)_i = A_{cf,i}\left(0.5b_w + d_{c,i}\right)$$

$$(Q_2)_i = (Q_1)_i + A_{cw,i}0.5\left(b_w + d_{c,i}\right)$$

$$(Q_3)_i = A_{c,i}0.5\left(b_w + d_{c,i}\right)$$

$$(Q_4)_i = (Q_3)_i + \frac{(b_w)^2}{8} w_{i,eff}$$

$A_{cw,i}$ is the area of each column web at storey i; $A_{cf,i}$ is the area of the each column flange at storey i; $A_{c,i}$ is the area of each column at storey i; $w_{i,eff}$ is the effective infill plate thickness at storey i; and $w_{c,i}$ is the web thickness of each column at storey i.

The effective infill plate thickness in every storey can be calculated based on the equation provided in both S16-09 and AISC 2010.

$$w_{i,eff} = \frac{1 - \frac{\pi}{4}\left(\frac{D}{S_{diag}}\right)}{1 - \frac{\pi}{4}\left(\frac{D}{S_{diag}}\right)\left(1 - \frac{N_r D \sin\alpha}{H_{c,i}}\right)} t_{w,i} \tag{8}$$

where $H_{c,i}$ is the clear column height between beam flanges at storey i; N_r is number of horizontal rows of perforations at storey i; $t_{w,i}$ is infill plate thickness at storey i; α is angle of inclined strip.

At any storey i, the equivalent moment of inertia for the P-SPSW, $I_{SW,i}$, is calculated as

Table 8 Shear-flexure properties for 4-storey P-SPSW

Storey	Column sections	Moment of inertia, I_{SW} (mm^4)	Effective shear area A_V (mm^2)
1	W360x509	$1.090 x 10^{12}$	16325
2	W360x509	$1.089 x 10^{12}$	15725
3	W360x314	$6.815 x 10^{11}$	15655
4	W360x314	$6.815 x 10^{11}$	15655

Table 9 Fundamental periods evaluated by two different analytical models

Storey	Fundamental period (sec)	
	Shell element model	Simple shear-flexure beam model
4-storey	1.01	1.0
8-storey	2.10	1.99
12-storey	3.27	3.10

$$I_{SW,i} = \frac{w_{i,eff}}{12}\left(L - d_{c,i}\right)^3 + 2I_{c,i} + \frac{1}{2}A_{c,i}(L)^2 \qquad (9)$$

where $I_{c,i}$ is the moment of inertia of each column at storey i.

Equivalent shear areas and moments of inertia in every storey were determined using the method described above. Table 8 presents the shear-flexure properties for 4-storey P-SPSW. The three selected P-SPSWs (4-, 8-, and 12-story) were fixed at the bases of the columns. With known shear and flexural properties for the equivalent beams at every floor, frequency analyses of the three equivalent shear-flexure cantilevers were carried out to determine their fundamental periods. Table 9 shows a comparison of the fundamental periods obtained from the simple shear-flexure cantilever models to the fundamental periods obtained from the detailed finite element models in ABAQUS. It is observed that the fundamental periods obtained from the simplified shear-flexure beam models are in good agreement with the fundamental periods obtained from the shell element models. The maximum difference between the two predictions is only 5.2%, obtained for the 12-storey SPSW. Thus, the simplified shear-flexure model can be used for determination of fundamental periods of P-SPSWs.

7. Conclusions

Nonlinear dynamic analyses have been performed to study the performance of code designed 4-storey, 8-storey and 12-storey P- SPWs. The applicability of the strip model currently used for solid unstiffened SPSW was also evaluated in this research for unstiffened P-SPSW. Furthermore, the effectiveness of a simple shear-flexure cantilever model to determine the fundamental period of P-SPSWs was also studied. The main findings of the study are summarized as follows:

(1) The detailed finite element model developed in this study was able to provide reasonably accurate predictions of the behaviour of P-SPSW. Excellent agreement was observed between test results and results from both quasi-static pushover and cyclic analyses.

(2) When subjected to earthquake records, code designed P-SPSWs showed excellent structural performance in terms of stiffness and ductility. For all earthquake records, all the P-SPSWs behaved in a robust manner: yielding was observed mainly in the perforated infill plates and the boundary columns and beams remained essentially elastic. For few cases partial yielding was observed in the columns at the base. For 8-storey and 12-storey P-SPSWs perforated infill plates at the top floors were only partially yielded. This was mainly because of use of minimum plate thickness of 3 mm. The theoretical required infill plate thickness for an optimal design was too thin to be practical.

(3) Interstorey drifts obtained from inelastic time history analyses were less than interstorey drift limit specified by NBC 2010. The infill plates at the upper levels were designed with overstrengths much greater than those at the lower storeys. Infill plates with high overstrength do not contribute much to the overall ductility. Thus, the seismic drift demands on the upper stories were less. It should be noted that although NBCC 2010 is used in this study and new building code NBCC 2015 now available, conclusions obtained from this study will remain same. This is because the inter-storey drift limit in NBCC 2015 remains same (2.5%) as NBCC 2010. Also, the seismic force modification factors, ductility related force modification factor (R_d) and overstrength related force modification factor (R_0), used for design of P-SPSWs did not change between NBCC 2010 and current NBCC 2015.

(4) It was observed from NTHA that the current code equation provided a good estimation of the shear strength of the perforated plate when the infill plate was fully yielded, especially near the base. Thus, for design of perforated SPSW, the current code equation of CSA/CAN S16-09 (same in S16-14) can be considered adequate.

(5) In addition, modified strip model was found to provide good predictions of nonlinear responses for P-SPSWs when tension strips have widths equal to distance between centre to centre (C/C) of perforations. In addition, exact layout of strips is recommended for modified strip model of perforated SPSW.

(6) The simplified shear-flexure beam model presented in this paper provides good estimation of the fundamental periods of P-SPSWs. The periods obtained from the shear-flexure models are slightly lower (maximum 5.2% for 12-storey P-SPSW) than the periods obtained from the detailed FE models. The slightly lower estimation provided by shear-flexure model would provide conservative estimate of base shear for seismic design. Thus, the simplified shear-flexure model can be used for

determination of fundamental periods of P-SPSWs. It is however recognised that the shear-flexure model presented in this paper is evaluated only for limited number of code designed perforated shear walls. More analysis of perforated SPSWs with a variation in geometry is required.

Acknowledgments

Funding for this research project is provided by the Faculty of Engineering and Computer Science, Concordia University, Montreal, Canada and the Natural Sciences and Engineering Research Council of Canada. Their financial support is acknowledged with thanks.

References

Ali, M.M., Osman, S.A., Husam, O.A. and Al-Zand, A.W. (2018), "Numerical study of the cyclic behavior of steel plate shear wall systems (SPSWs) with differently shaped openings", *Steel Compos. Struct., Int. J.*, **26**(3), 361-373.

ANSI/AISC (2010), Seismic Provisions for Structural Steel Buildings; American Institute of Steel Construction, Chicago, IL, USA.

ANSI/AISC 360-16 (2016), Specifications for Structural Steel Buildings; American Institute of Steel Construction, Chicago, IL, USA.

ASCE 7-10 (2010), Minimum Design Loads for Buildings and Other Structures; American Society of Civil Engineers, Structural Engineering Institute, USA.

Atkinson, G.M. (2009), Earthquake Time Histories Compatible with the 2005 NBCC Uniform Hazard Spectrum.
URL: www.seismotoolbox.ca

Barkhordari, M.A., Hosseinzadeh, S.A.A. and Seddighi, M. (2014), "Behavior of steel plate shear walls with stiffened full-height rectangular openings", *Asian J. Civil Eng.*, **15**(5), 741-759.

Barua, K. (2016), "Seismic performance of perforated steel plate shear walls designed according to Canadian seismic provisions", M.Sc. Thesis; Concordia University, Montreal, QC, Canada.

Berman, J.W. and Bruneau, M. (2008), "Capacity design of vertical boundary elements in steel plate shear walls", *Eng. J.*, **45**(1), 57-71.

Bhowmick, A.K., Driver, R.G. and Grondin, G.Y. (2009), "Seismic analysis of steel plate shear walls considering strain rate and P–delta effects", *J. Constr. Steel Res.*, **65**(5), 1149-1159.

Bhowmick, A.K., Grondin, G.Y. and Driver, R.G. (2011), "Estimating fundamental periods of steel plate shear walls", *Eng. Struct.*, **33**, 1883-1893.

Bhowmick, A.K., Grondin, G.Y. and Driver, R.G. (2014), "Nonlinear seismic analysis of perforated steel plate shear walls", *J. Constr. Steel Res.*, **94**, 103-113.

Charney, F.A., Iyer, H. and Spears, P.W. (2005), "Computation of major axis shear deformations in wide flange steel girders and columns", *J. Constr. Steel Res.*, **61**, 1525-1558.

CSA (2009), Limit states design of steel structures; Canadian Standards Association, CAN/CSA-S16-09, Toronto, ON, Canada.

CSA (2014), Limit States Design of Steel Structures; Canadian Standards Association, CAN/CSA-S16-14, Mississauga, ON, Canada.

Driver, R.G., Kulak, G.L., Kennedy, D.J.L. and Elwi, A.E. (1998), "Cyclic test of four storey steel plate shear wall", *J. Struct. Eng.*, ASCE, **124**(2), 112-120.

Gail, A., Karen, A. and Bernie, D. (2009), Engineering seismology toolbox.

Hibbitt, Karlsson, and Sorensen (2007), ABAQUS/Standard User's Manual; Version 6.7, HKS Inc., Pawtucket, RI, USA.

Hosseinzadeh, S.A.A. and Tehranizadeh, M. (2012), "Introduction of stiffened large rectangular openings in steel plate shear walls", *J. Constr. Steel Res.*, **77**, 180-192.

Naumoski, N., Saatcioglu, M. and Amiri-Hormozaki, K. (2004), "Effects of scaling of earthquake excitations on the dynamic response of reinforced concrete frame buildings", *Proceedings of the 13th World Conference on Earthquake Engineering*, Vancouver, BC, Canada.

NBCC (2010), National Building Code of Canada. Canadian Commission on Building and Fire Codes; National Research Council of Canada (NRCC), Ottawa, ON, Canada.

PEER (2010), Next Generation Attenuation of Ground Motions Project (NGA) Database; Pacific Earthquake Engineering Research Center, Berkely, CA, USA.

Purba, R.H. (2006), "Design recommendations for perforated steel plate shear walls", M.Sc. Thesis; State University of New York at Buffalo, NY, USA.

Qu, B. and Bruneau, M. (2010), "Capacity design of intermediate horizontal boundary elements of steel plate shear walls", *J. Struct. Eng.*, **136**(6), 665-675.

Roberts, T.M. and Sabouri-Ghomi, S. (1992), "Hysteretic characteristics of unstiffened perforated steel plate shear panels", *Thin-Wall. Struct.*, **14**, 139-151.

Sabouri-Ghomi, S. and Mamazizi, S. (2015), "Experimental investigation on stiffened steel plate shear walls with two rectangular openings", *Thin-Wall. Struct.*, **86**, 56-66.

Sabouri-Ghomi, S., Mamazizi, S. and Alavi, M. (2016), "An Investigation into Linear and Nonlinear Behavior of Stiffened Steel Plate Shear Panels with Two Openings", *Adv. Struct. Eng.*, **18**(5), 687-700.

Shekastehband, B., Azaraxsh, A.A. and Showkati, H. (2017), "Hysteretic behavior of perforated steel plate shear walls with beam-only connected infill plates", *Steel Compos. Struct., Int. J.*, **25**(4), 505-521.

Shishkin, J.J., Driver, R.G. and Grondin, G.Y. (2005), "Steel plate shear walls using the modified strip model", Structural Engineering Report No. 261; Department of Civil and Environmental Engineering, University of Alberta, Edmonton, AB, Canada.

Soltani, N., Abedi, K., Poursha, M. and Golabi, H. (2017), "An investigation of seismic parameters of low yield strength steel plate shear walls", *Eartq. Struct., Int. J.*, **12**(6), 713-723.

Thorburn, L.J., Kulak, G.L. and Montgomery, C.J. (1983), "Analysis of Steel Plate Shear Walls", Structural Report No. 107; Department of Civil and Environmental Engineering, University of Alberta, Edmonton, AB, Canada.

Topkaya, C. and Kurban, C.O. (2009), "Natural periods of steel plate shear wall systems", *J. Constr. Steel Res.*, **65**(3), 542-551.

Vian, D. (2005), "Steel plate shear wall for seismic design and retrofit of building structures", Ph.D. Thesis; The state university of New York at Buffalo, NY, USA.

DL